

Supporting Information

Ultra-Low-Temperature Ozone Abatement on α -MnO₂(001) Facets with Down-Shifted Lowest Unoccupied Orbitals

Yaxin Chen,[†] Weiye Qu,[†] Chao Li,[†] Junxiao Chen,[†] Zhen Ma,^{†,‡} and Xingfu Tang^{*,†,‡}

[†] Shanghai Key Laboratory of Atmospheric Particle Pollution & Prevention (LAP³), Department of Environmental Science & Engineering, Fudan University, Shanghai 200433, China

[‡] Shanghai Institute of Pollution Control & Ecological Security, Shanghai 200092, China

Tel: +86-21-31248935. E-mail: tangxf@fudan.edu.cn

Pages S1-S11

Methods in detail

Tables S1-S2

Figures S1-S7

Contents

Methods in detail

Table S1. Specific surface areas of α -MnO₂ sheet, α -MnO₂ rod, and β -MnO₂.

Table S2. EXAFS parameters of α -MnO₂ sheet and α -MnO₂ rod at the Mn *K*-edge.

Figure S1. XRD patterns of α -MnO₂ sheet and α -MnO₂ rod.

Figure S2. HRTEM image of α -MnO₂ sheets.

Figure S3. $\chi(R)$ k^2 -weighted FT EXAFS spectra at the Mn *K*-edge of α -MnO₂ sheet and α -MnO₂ rod.

Figure S4. *R*-space and inverse FT spectra at the Mn *K*-edge of α -MnO₂ sheet and α -MnO₂ rod.

Figure S5. X-ray absorption spectra of α -MnO₂ sheet and α -MnO₂ rod at the Mn *K*-edge.

Figure S6. X_{O_3} as a function of temperature (*T*) over α -MnO₂ sheets.

Figure S7. Valence-band XPS of α -MnO₂ sheets and β -MnO₂.

Materials and methods in detail

Catalytic Evaluation. The catalytic performance for ozone removal was evaluated in a fixed-bed quartz reactor (i.d. = 8 mm) under an atmospheric pressure, using 0.2 g catalyst (40–60 mesh) for each run. Data were recorded by a temperature-programmed mode at a ramping rate of 2 °C min⁻¹. O₃ was generated using ozonator (Guangdong Chuanghuan Ozone Electric Equipment Company, China). The total flow rate through the reactor was maintained at 1.7 L/min (0.5 vol% O₂ and Ar balance) and the inlet ozone concentration maintained at ~60 ppm. The ozone concentration was determined with an ozone analyzer (Model 49i, Thermo Scientific, USA).

Material Characterization. X-ray diffraction (XRD) patterns were obtained at a Rigaku Ultima-IV diffractometer (Japan) with Cu K α radiation (λ = 1.5406 Å). Transmission electron microscopy (TEM) and high-resolution TEM (HRTEM) studies were conducted on a JEM 2100F transmission electron microscope. XANES and EXAFS spectra were obtained at the Mn *K*-edges at BL14W of the SSRF with an electron beam energy of 3.5 GeV and a ring current of 200–300 mA. Data were collected with a fixed exit monochromator using two flat Si(111) crystals for the *K*-edge XAS measurements. The raw data were analyzed by using the IFEFFIT 1.2.11 software package. Soft X-ray absorption spectra at the Mn *L*₃-edges were obtained in a total electron yield (TEY) mode at the 4B9B of the Beijing Synchrotron Radiation Facility (BSRF). X-ray photoelectron (XPS) spectra were obtained at BL 4B9B in the BSRF at a photon energy of 780 eV. All the data were recorded in an ultrahigh vacuum chamber equipped with a VG Scienta R4000 electron energy analyzer with a base pressure of $\sim 4 \times 10^{-11}$ mbar at room temperature. BE of these valence-band spectra were calibrated with respect to the Au 4f_{7/2} (BE = 84 eV) featured from a clean gold foil attached to the manipulator. The specific surface areas (SBET) were determined by using linear portion of Brunauer–Emmett–Teller (BET) model. The BET surface areas were measured by N₂ adsorption at a liquid nitrogen temperature using a NOVA4000e (USA, Quantachrome) automated gas sorption system.

Tables and Figures

Table S1. Specific surface areas of α -MnO₂ sheet, α -MnO₂ rod, and β -MnO₂.

Samples	α -MnO ₂ sheet	α -MnO ₂ rod	β -MnO ₂
$S_{\text{BET}}/(\text{m}^2/\text{g})$	76	59	15

Table S2. EXAFS parameters of α -MnO₂ sheet and α -MnO₂ rod at the Mn *K*-edge.

Samples	Shell	CN ^[a]	R ^[b] / Å	σ^2 ^[c] / Å ²	ΔE_0 ^[d] / eV
α -MnO ₂ sheet	Mn-O	6	1.90(5)	0.005(7)	2.1
	Mn-Mn	3.2	2.82(4)	0.007(6)	-4.9
α -MnO ₂ rod	Mn-O	6	1.88(7)	0.005(3)	-0.1
	Mn-Mn	4	2.90(4)	0.008(3)	0.03

R -space fit, $\Delta k = 2\text{-}12.3 \text{ \AA}^{-1}$, $\Delta r = 1.1\text{-}4 \text{ \AA}$;

^[a] CN , coordination number;

^[b] R , distance between absorber and backscatter atoms;

^[c] σ^2 , Debye-Waller factor;

^[d] ΔE_0 , energy shift.

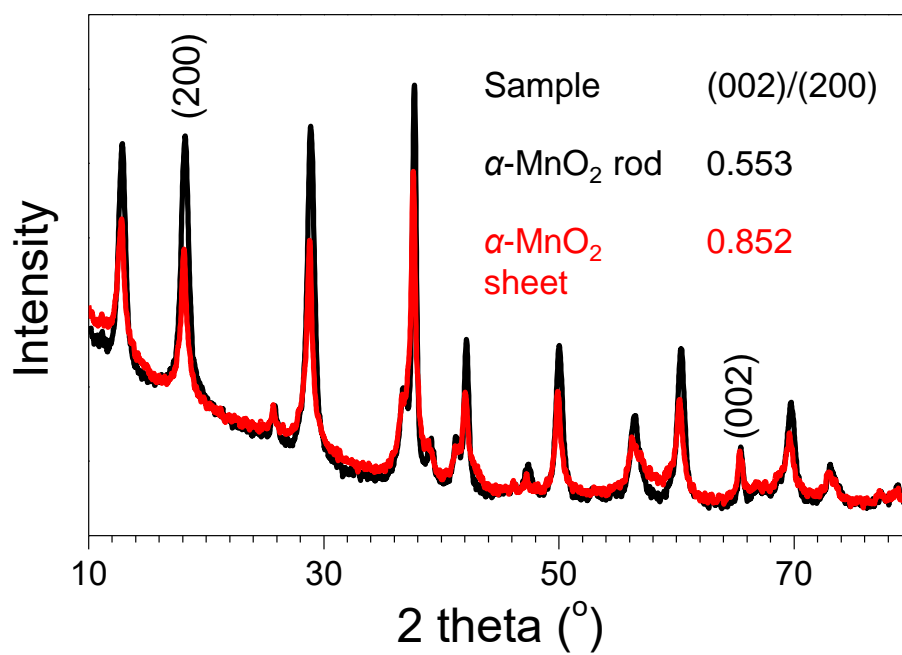


Figure S1. XRD patterns of α -MnO₂ sheet and α -MnO₂ rod. Inset: The ratios of FWHM between (002) and (200) diffraction peaks.

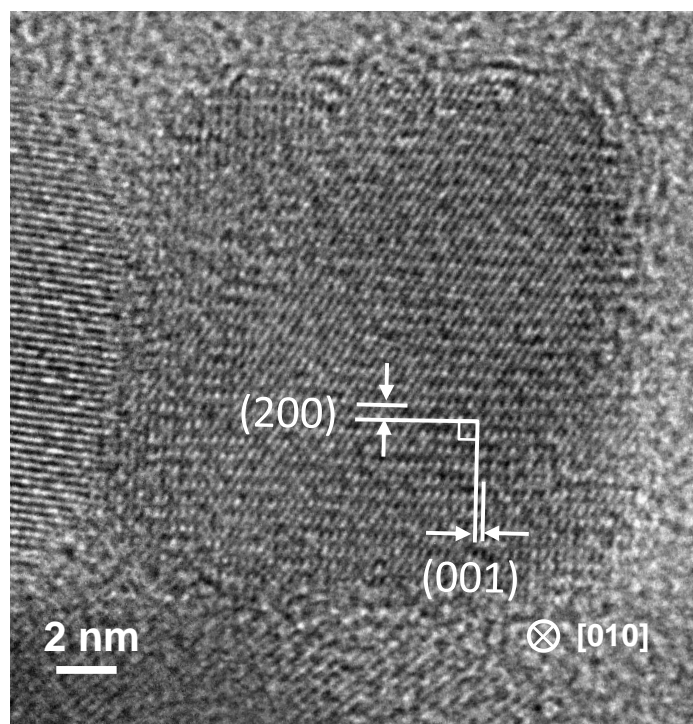


Figure S2. HRTEM image of α -MnO₂ sheets.

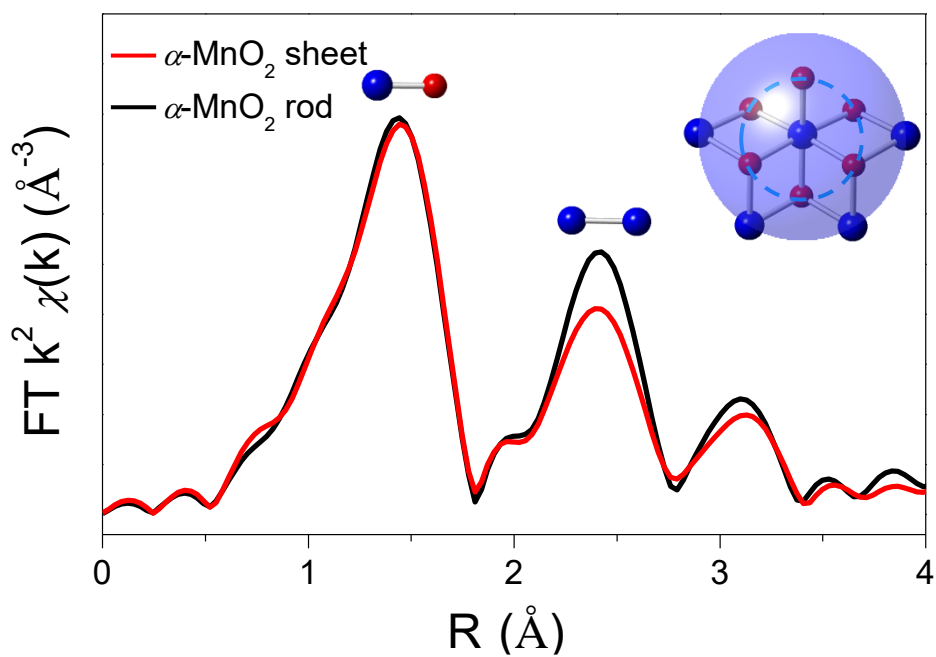


Figure S3. $\chi(R)$ k^2 -weighted FT EXAFS spectra at the Mn K -edge of α -MnO₂ sheet and α -MnO₂ rod.

Blue and red balls represent Mn and O atoms, respectively. The inset models shows four Mn atoms (blue) and six O atoms (red) within a shell with a radius of approximately 3.0 \AA of the Mn center.

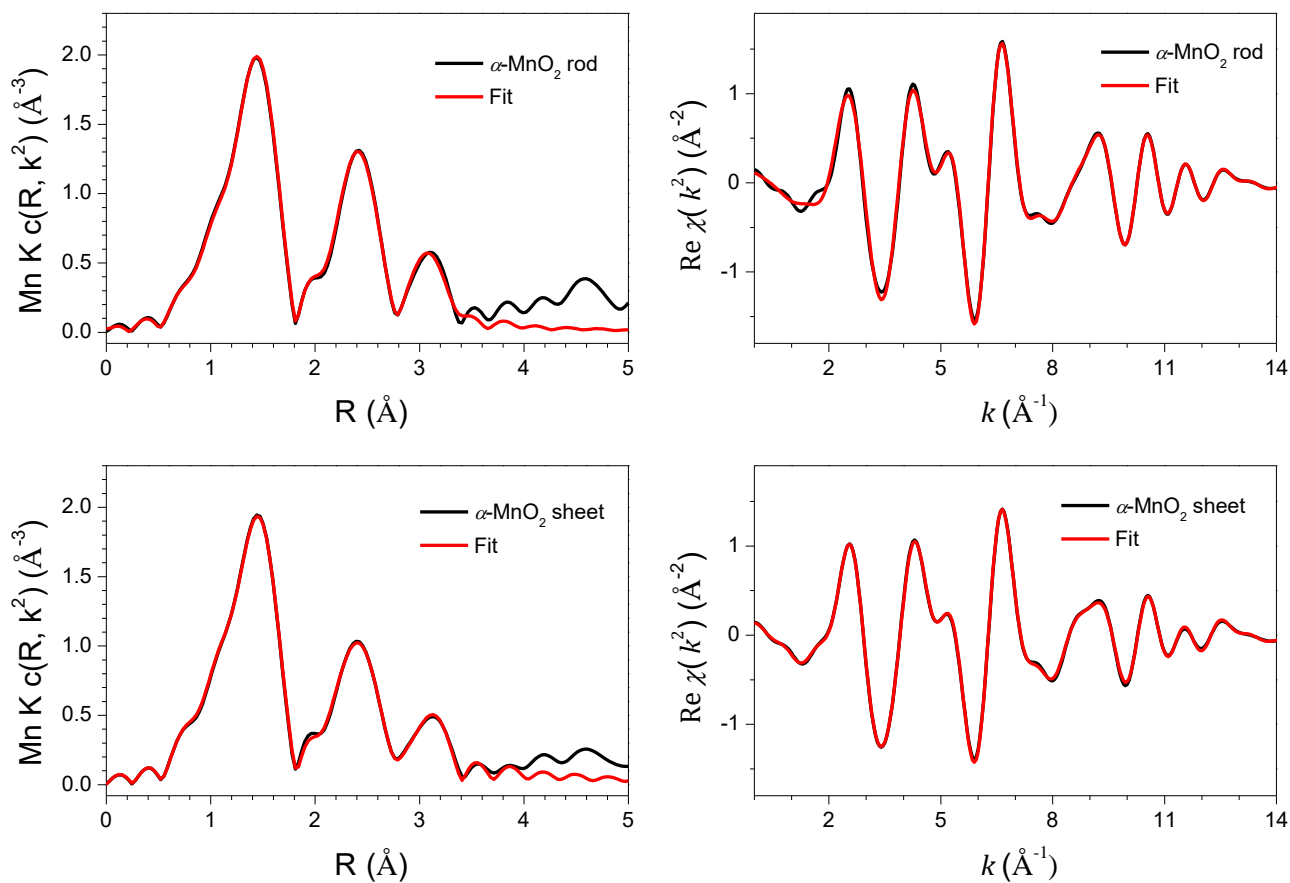


Figure S4. R -space ($\Delta k = 2\text{-}12.3 \text{\AA}^{-1}$) and inverse FT spectra ($\Delta r = 1.1\text{-}4.0 \text{\AA}$) at the Mn K -edge of α -MnO₂ sheet and α -MnO₂ rod.

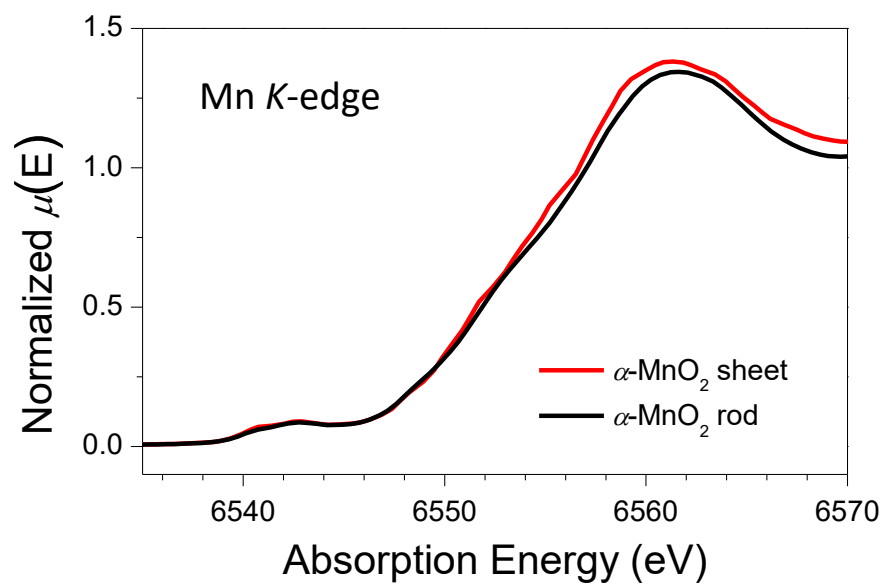


Figure S5. X-ray absorption spectra of α -MnO₂ sheet and α -MnO₂ rod at the Mn K-edge.

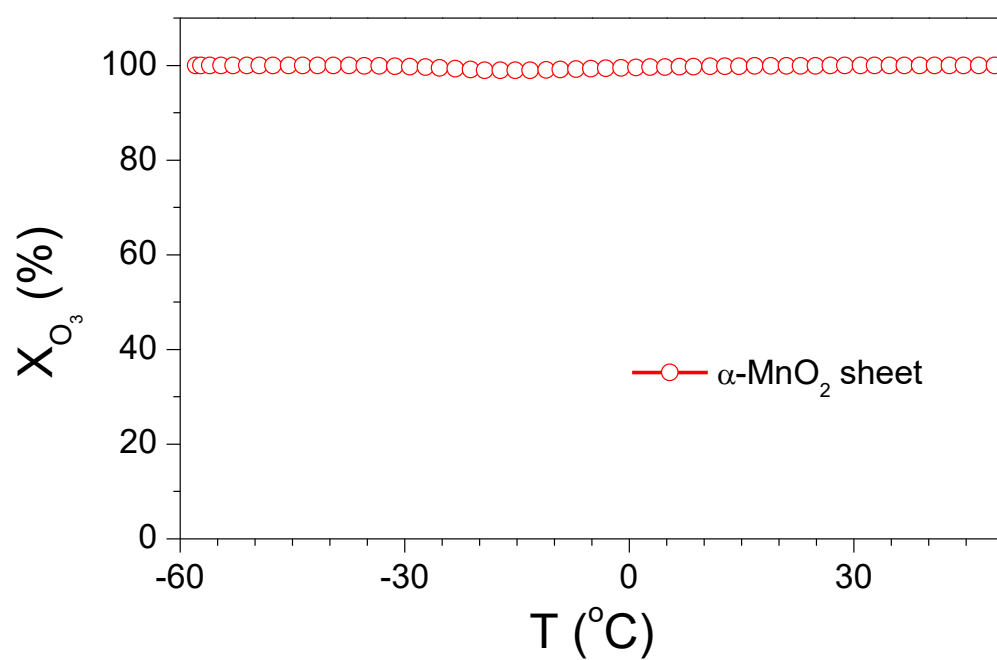


Figure S6. X_{O_3} as a function of temperature (T) over α - MnO_2 sheets. Reaction Conditions: 60 ppm O_3 , 0.5 vol% O_2 and Ar balance, gaseous hourly space velocity 460,000 h^{-1} .

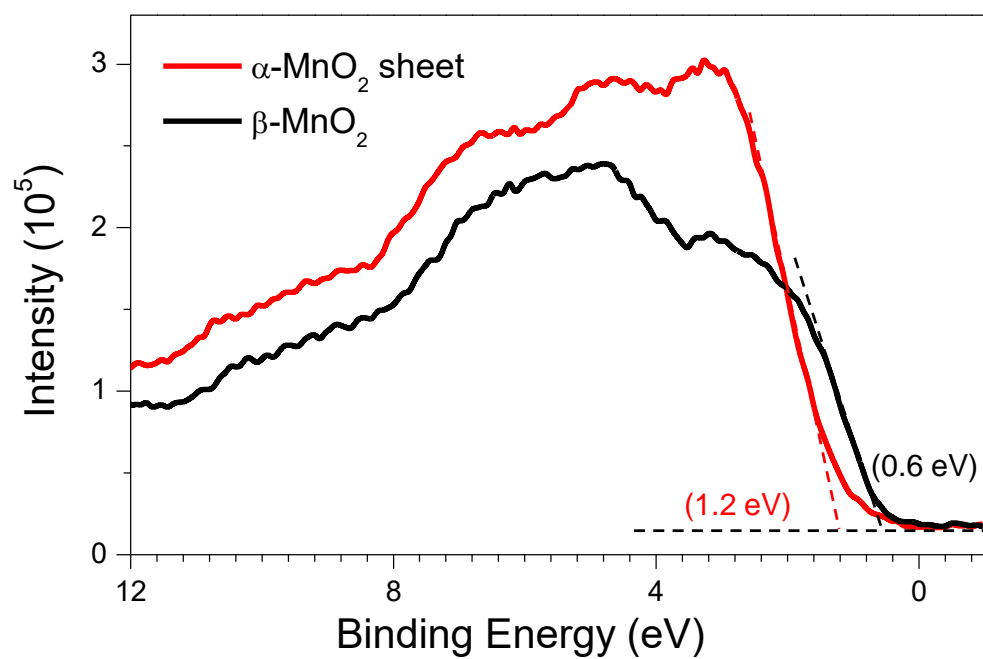


Figure S7. Valence-band XPS of α -MnO₂ sheets and β -MnO₂.